Article

pubs.acs.org/Biomac

Ligand-Induced Cross-Linking of Z-Elastin-like Polypeptide-Functionalized E2 Protein Nanoparticles for Enhanced Affinity Precipitation of Antibodies

Andrew R. Swartz, Qing Sun,[†] and Wilfred Chen*

Department of Chemical and Biomolecular Engineering, University of Delaware, Newark, Delaware 19716, United States

Supporting Information

ABSTRACT: Affinity precipitation is an ideal alternative to chromatography for antibody purification because it combines the high selectivity of an affinity ligand with the operational benefits of precipitation. However, the widespread use of elastin-like polypeptide (ELP) capture scaffolds for antibody purification has been hindered by the high salt concentrations and temperatures necessary for efficient ELP aggregation. In this paper, we employed a tandem approach to enhance ELP aggregation by enlarging the dimension of the capturing scaffold and by creating IgG-triggered scaffold cross-linking. This was accomplished by covalently conjugating the Z-domain-ELP (Z-ELP) capturing scaffold to a 25 nm diameter E2 protein nanocage using Sortase A ligation. We demonstrated the isothermal recovery of IgG in the virtual absence of salt due to the significantly increased scaffold dimension and cross-linking from multivalent IgG−E2 interactions. Because IgG cross-linking is reversible at low pH, it may be feasible to achieve a high yielding IgG purification by isothermal phase separation using a simple pH trigger.

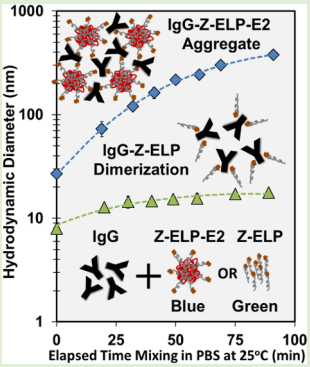

INTRODUCTION

Monoclonal antibodies (mAbs) represent a rapidly expanding class of biopharmaceutical therapeutics,[1] and the global market is expected to exceed $120 billion by 2020.[2] This increasing demand has placed a significant burden on the downstream purification platform. The initial capture step, Protein A affinity chromatography, has been especially impacted due to limitations in throughput, scale-up, and cost.[3,4] This bottleneck has generated increased interest in non-chromatographic capture technologies.

Affinity precipitation is an ideal alternative to chromatography because it combines the high selectivity of an affinity ligand with the operational benefits of precipitation.[5] Thermally responsive synthetic polymers have been implemented for antibody affinity precipitation, but the production of these polymers require tedious and expensive chemical synthesis steps.[6,7] In contrast, elastin-like polypeptides (ELPs) are environmentally responsive biopolymers that can be easily produced by recombinant hosts,[8,9] and a wide range of binding partners has been genetically fused to ELP without impacting either the inverse phase transition property or the affinity interaction.[10−13]

We have previously fused a small (7 kDa) immunoglobulin G (IgG)-binding Z-domain derived from Protein A to ELP (Z-ELP) for mAb purification.[14] However, this system was limited by the high salt concentrations and temperatures necessary to ensure the formation of large, insoluble aggregates for efficient recovery by centrifugation. In addition, exposure to these harsh solution conditions resulted in increased mAb aggregation and loss of activity.[15−17] One way to achieve larger aggregate sizes without salt or temperature is to enlarge the dimension and valency of the capturing scaffold.[18,19] Our group has recently demonstrated the feasibility of attaching multiple proteins onto the E2 core of the pyruvate dehydrogenase complex from *Bacillus stearothermophilus*, a genetically modifiable, thermostable 25 nm diameter 60-mer protein nanocage, by Sortase A (SrtA)-mediated ligation.[20] SrtA is ideal for conjugating biomolecules because it is active at mild solution conditions, utilizes small N (GGG-) and C (-LPETG) terminal recognition motifs, and is easily expressed in *Escherichia coli*.[21] We hypothesize that ligating Z-ELP onto E2 nanocages will enable the precipitation of bound IgG at much lower salt concentrations and/or temperatures because of the significantly increased dimension and cross-linking from multivalent IgG−nanocage interactions (Figure 1).

EXPERIMENTAL SECTION

Materials. *E. coli* strain BLR(DE3) containing pET24(a) vectors encoding for Z-ELP[KV_8F-40]-LPETG and ELP[KV_8F-40]-LPETG were constructed and described previously.[22] *E. coli* strain BL21(DE3) containing a pET11(a) vector encoding for GGG-E2(158) and another BL21(DE3) strain containing a pMR5 vector encoding for SrtA enzyme were constructed and described previously.[20] Human polyclonal IgG and fluorescein isothiocyanate (FITC) conjugated human IgG were purchased from Sigma-Aldrich (St. Louis, MO). Bacto tryptone and yeast extract were purchased from BD Biosciences (Franklin Lakes, NJ). Glycerol, kanamycin, ampicillin, isopropyl-β-D-thiogalactoside (IPTG), calcium chloride, and sodium chloride were purchased from Fisher Scientific (Pittsburgh, PA). Sodium hydroxide,

Received: February 23, 2017
Revised: March 31, 2017
Published: April 4, 2017

DOI: 10.1021/acs.biomac.7b00275
Biomacromolecules 2017, 18, 1654−1659

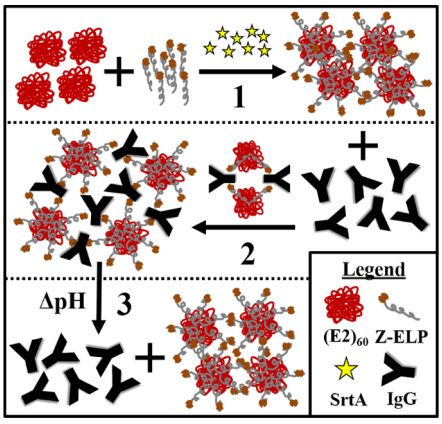

Figure 1. Enhanced affinity precipitation of IgG using Z-ELP-E2 nanoparticles through a combination of increased aggregate sizes and cross-linking via multivalent interactions. Step 1: Sortase A ligation of Z-ELP onto E2 60-mer nanocage. Step 2: Multivalent binding between the nanoparticles and IgG result in spontaneous cross-linking and formation an insoluble precipitate. Step 3: Reversible dissociation and resolubilization of both IgG and Z-ELP-E2 in a low pH buffer.

potassium mono- and dibasic phosphate, sodium phosphate dibasic, bovine serum albumin (BSA), L-arginine, tris base, and ammonium sulfate were purchased from Sigma-Aldrich. Vivaspin 20 columns (100 kDa) were purchased from Sartorius Stedim (Gottingen, Germany).

Protein Expression and Purification. Z-ELP[KV_8F-40]-LPETG and ELP[KV_8F-40]-LPETG were expressed in BLR(DE3) *E. coli* cells grown in Terrific Broth medium (TB) with 50 μg/mL kanamycin at 37 °C and 250 rpm for 24 h with leaky expression. SrtA was expressed in BL21(DE3) *E. coli* cells grown in Luria−Bertani Medium (LB) with 50 μg/mL kanamycin at 37 °C and 250 rpm until an OD600 of 1.0, where the culture was induced with 1 mM IPTG and subsequently incubated at 37 °C for 4 h. GGG-E2 was expressed in BL21(DE3) *E. coli* cells grown in LB with 100 μg/mL ampicillin at 37 °C and 250 rpm until an OD600 of 0.5, where the culture was induced with 0.2 mM IPTG and subsequently incubated at 20 °C for 20 h. After protein expression, all cultures were harvested by centrifugation at 4000*g* for 15 min at 4 °C and resuspended in a tris buffer (50 mM Tris, 150 mM sodium chloride, pH 8.0). Cells were lysed using a Fisher Sonicator (Pittsburgh, PA) using 5 s pulse on and 10 s pulse off for 10 min over ice. Soluble lysate was separated by centrifugation at 15 000*g* for 20 min at 4 °C. ELPs were purified using 2−3 rounds of inverse transition cycling (ITC) as described previously[9] using 0.5 M ammonium sulfate for precipitation and were resuspended in the tris buffer. Molar concentration of purified ELP was determined by measuring absorbance at 280 nm on a Shimadzhu UV-1800 spectrophotometer (Kyoto, Japan). The thermostable GGG-E2 cage was purified by incubating at 70 °C for 10 min to precipitate contaminant proteins. The soluble E2 was separated by centrifugation at 15 000*g* for 15 min. Total protein concentration of purified GGG-E2 and soluble SrtA lysate were measured by Bradford protein assay purchased from Bio-Rad (Hercules, CA) using BSA as a standard. Protein expression was confirmed by Coomassie stained, 10% acrylamide sodium dodecyl sulfate polyacrylamide gel electrophoresis (SDS-PAGE) using a Bio-Rad Mini-PROTEAN electrophoresis system (Hercules, CA) (Supporting Information, Figure S1). Protein purity was estimated using densitometry analysis of SDS-PAGE gels using Thermo MyImage software (Waltham, MA).

Sortase A Mediated Ligation. Ligation of ELP-LPETG or Z-ELP-LPETG to the E2 cage was catalyzed by the SrtA enzyme. Target molar ratios of ELP-LPETG, GGG-E2, and SrtA were added to a reaction buffer consisting of 50 mM tris, 150 mM sodium chloride, and 6 mM calcium chloride, pH 8.0 in a centrifuge tube. The reaction mixture was incubated at 37 °C for 4 h. The ligation product was purified using one round of ITC using 1 M ammonium sulfate and was resuspended in phosphate buffered saline (PBS; 137 mM NaCl, 2.7 mM KCl, 10 mM Na_2HPO_4, and 2 mM KH_2PO_4, pH 7.4). The excess, unreacted ELP was removed by 100 kDa diafiltration into PBS using Sartorius Vivaspin 20 spin columns. The purified Z-ELP-E2 or ELP-E2 nanocage was confirmed by Coomassie stained 10% acrylamide SDS-PAGE (Supporting Information, Figure S2), and ELP ligation density was estimated using densitometry analysis using Thermo MyImage software (Waltham, MA). The ligation products were characterized by transition temperature (T_t) evaluated using UV spectroscopy on a Shimadzhu UV-1800 spectrophotometer (Kyoto, Japan), by dynamic light scattering (DLS) using a Malvern Zetasizer Nano (Malvern, United Kingdom) with a 4 mW He Ne gas laser at 632.8 nm and a 175° scattering angle (Supporting Information, Figure S3C) and by transmission electron microscopy (TEM) with a Zeiss Libra 120 Electron Microscope (Oberkochen, Germany) using 2% uranyl acetate staining on a carbon coated grid from Electron Microscopy Sciences (Hatfield, PA) (Supporting Information, Figures S3A and S3B). All statistical analyses were performed using Minitab 17 (State College, PA).

Transition Temperature Measurement. Equal concentrations of free Z-ELP and ligated Z-ELP were prepared at 4 °C in PBS with target ammonium sulfate concentrations (0, 0.1, 0.2, 0.3, and 0.5 M) or with human polyclonal IgG at a 5:1 Z:IgG molar ratio and were incubated either at 4 or 20 °C for 1−2 h. After the incubation time, samples were added to an 8-well multicell 100 μL microcuvette (Shimadzhu), and the absorbance at 350 nm was measured every 0.5 degrees from either 4−50 or 20−65 °C at a ramp rate of 0.5 degree per min with a 20 s equilibration before each measurement. Three separate measurements were performed for each condition, and T_t was calculated by evaluating the maximum slope of the transition curve. T_t and absorbance profile analyzed by the provided Tm Analysis Software (Shimadzhu) was extracted from each measurement. Two-sample *t*-tests were employed to determine the statistical significance of the hypothesized difference of T_t values.

Dynamic Light Scattering Measurement. Three replicate DLS measurements were taken using a low volume cuvette (ZEN0040, Malvern) for each sample consisting of 5 runs of 10 s using the settings sample = protein (RI = 1.45, absorption = 0.001), and dispersant = water (RI = 1.33). The correlation function was analyzed by the Protein Analysis algorithm provided by the Malvern software. The hydrodynamic diameter (Z-ave), polydispersity index, and volume distributions were extracted from each measurement. For the kinetic experiments, equal concentrations of both free Z-ELP and Z-ELP ligated to E2 cages were prepared with a human polyclonal IgG at a 5:1 Z:IgG molar ratio in PBS at 25 °C. Samples containing free ELP (with no Z-domain) and ELP ligated to E2 cage were also prepared with IgG at a 5:1 ratio as a control. Immediately after each sample was prepared, the hydrodynamic radius was measured at 25 °C and then measured again at approximately 10−20 min intervals over the next 90 min while keeping all samples at 25 °C. For all other DLS experiments, samples were prepared in PBS with target ammonium sulfate concentrations or with IgG at a 5:1 Z:IgG molar ratio and incubated at 23 °C for 1−2 h before each measurement.

Antibody Affinity Precipitation. IgG affinity precipitation yield was compared between free Z-ELP and Z-ELP ligated to the E2 nanocage at different salt concentrations. First, equal molar concentrations of free Z-ELP and ELP and ligated Z-ELP-E2 and ELP-E2 cages were mixed with human polyclonal IgG at a 5:1 molar ratio in PBS and incubated at 23 °C for 2 h in microcentrifuge tubes. ELP and ELP-E2 (no Z-domain) were used as controls. Second, the complex was precipitated using increasing concentrations of ammonium sulfate (0.1, 0.25, and 0.5 M) and incubated at 23 °C for 10 min. The solution was centrifuged for 10 min at 15 000*g* at 23 °C to pellet the precipitate. Third, the supernatant was removed, and the pellet was resuspended in elution buffer (0.5 M arginine, pH 3.7) and incubated for 1 h at 4 °C. A second precipitation was performed using 1 M ammonium sulfate for all arms to precipitate the ELP. Upon another centrifugation, the IgG was separated in the supernatant from the ELP in the pellet. Bradford assay was used to quantify IgG recoveries using a standard curve prepared with known IgG concentrations. All experimental samples were run in triplicate.

DOI: 10.1021/acs.biomac.7b00275
Biomacromolecules 2017, 18, 1654−1659

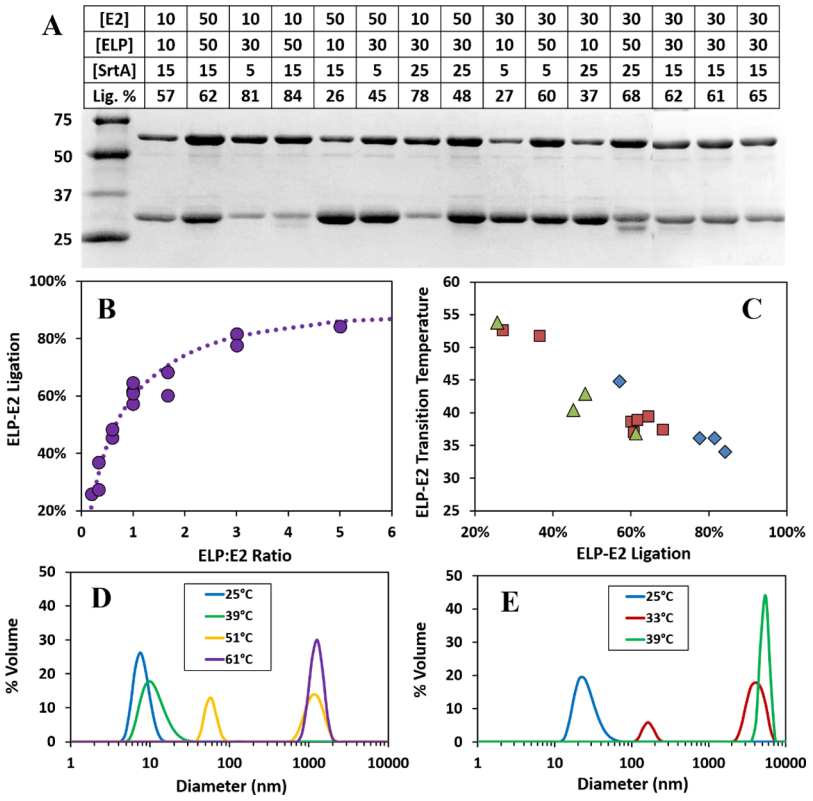

Figure 2. Nanocage ligation and aggregation properties. (A) SDS-PAGE analysis of purified nanocage ligation products produced from various reactant concentrations. Top band: ELP-E2 subunit (55 kDa). Bottom band: E2 subunit (29 kDa). (B) Dependency of ELP-E2 ligation density on ELP:E2 ratios. (C) Dependency of T_t on ELP-E2 ligation density normalized by E2 concentration (green triangle: 25 μM; red square: 15 μM; blue diamond: 5 μM). DLS % volume distribution of either (D) 25 μM free ELP or (E) 25 μM ELP ligated on E2 cages at 60% ligation density in PBS at selected temperatures.

Turbidity Measurement. Turbidity was measured by absorbance at 350 nm using a Synergy H4 microplate reader purchased from Biotek (Winooski, VT). Samples were prepared with equal concentrations of free and ligated Z-ELP and were mixed with human polyclonal IgG at a 5:1 molar ratio in PBS and incubated at 23 °C for 2 h in microcentrifuge tubes. After the initial incubation, samples were adjusted to 0.5 M ammonium sulfate and pelleted by centrifugation at 15 000*g*. Samples were resuspended back in PBS and incubated for 1 h and 3 days at 4 °C with mixing. After incubation, samples were precipitated with 0.5 M ammonium sulfate and pelleted by centrifugation at 15 000*g*. Samples were resuspended in the elution buffer and incubated at 23 °C for 15 min. Turbidity was measured immediately after each sample was taken. All samples were run in triplicate.

RESULTS AND DISCUSSION

Formation of Z-ELP-E2 Nanoparticles by Sortase A Ligation. To enable IgG binding, a new Z-ELP-LPETG fusion protein was created by adding the Z-domain to the N-terminus of ELP-LPETG.[22] A wide range of conditions was tested for expression, and the optimal productivity of >750 mg/L culture was achieved using leaky expression without IPTG addition at 37 °C (Supporting Information, Figure S1). Highly purified protein was obtained by two rounds of ITC as described previously.[9] GGG-E2 nanocages were expressed and partially purified by heating the cell lysates at 70 °C for 10 min as described before[20] (Supporting Information, Figure S1).

Sortase A ligation was performed by incubating the reactants for 4 h in pH 8 buffer with 6 mM $CaCl_2$ at 37 °C. The resulting product was purified using two ITC cycles and filtered using a 100 kDa membrane to remove unreacted ELP (Supporting Information, Figure S2). TEM and DLS were utilized to confirm the nanocage structure and size using the 60% ligation product as an example. TEM images of a single nanocage (Supporting Information, Figure S3A) and mixture of nanocages (Supporting Information, Figure S3B) depict the expected dodecahedron structure and size consistent with previous characterization.[23] From DLS analysis of 3 ligation products (Supporting Information, Figure S3C), the samples had a polydispersity <0.3 and an average hydrodynamic diameter of 34.5 ± 2.8 nm. These results indicate that a highly pure, monodisperse solution of Z-ELP-E2 nanocages can be consistently produced using the indicated procedures.

Characterizaton of Z-ELP-E2 Nanoparticles with Different Ligation Densities. We first investigated the impact of ELP-E2 conjugation density on phase transition properties. The initial ligation experiments were performed using ELP:E2 ratios ranging from 1:5 to 5:1 and varying SrtA concentrations. The percentage of Z-ELP ligated onto E2 varied from 25 to 85% as characterized by SDS-PAGE and quantified by densitometry (Figures 2A and B). T_t in the absence of any added salt (except 150 mM sodium chloride in the buffer) was calculated by measuring the absorbance at 350 nm over a temperature gradient from 20 to 60 °C. Consistent with our expectation, higher ELP-E2 ligation densities yielded lower T_t values (Figure 2C). T_t was reduced by 20 °C by increasing the ELP:E2 ligation density from 25 to 75%. The high ligation density E2 nanocages (≥60%) had a T_t over 20 °C less than free Z-ELP at the same protein concentration. To further investigate this observation, DLS measurements were

DOI: 10.1021/acs.biomac.7b00275
Biomacromolecules 2017, 18, 1654−1659

performed at the known baseline (0% precipitated), transition (50% precipitated), and peak (100% precipitated) temperatures for a 60% ligation product and free ELP (Figures 2D and E). Both samples were the expected size at baseline temperature and exhibited a bimodal distribution at T_t. At its peak temperature of 39 °C, the Z-ELP-E2 nanocage was over 2 orders of magnitude larger than Z-ELP at 39 °C and still significantly larger than Z-ELP at its peak temperature of 61 °C. These results support the conclusion that the formation of larger aggregates is a direct result of the enhanced dimension of the Z-ELP-E2 scaffold. Moreover, a higher ELP grafting density onto E2 may also increase the local hydrophobicity, resulting in coacervation at reduced temperatures.

It is well-known that T_t of ELP can be significantly lowered by salt addition. Using the 60% ligation Z-ELP-E2 product as an example, the transition property was measured over a wide range of ammonium sulfate concentrations (Figure 3A).

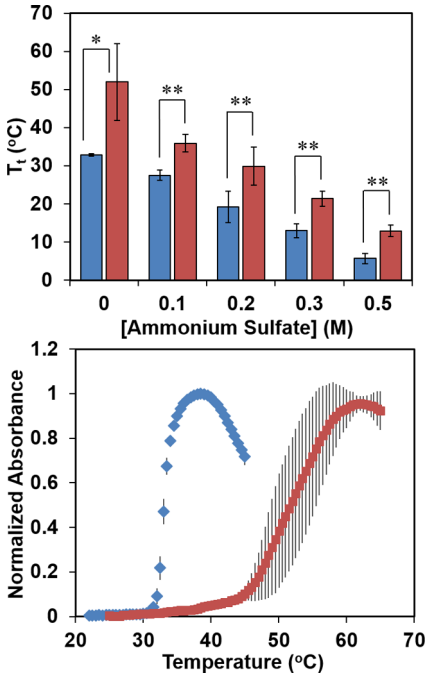

Figure 3. T_t comparison between 25 μM free ELP and ligated ELP on E2 cages at 60% ligation density. (A) T_t of the nanocage (blue) and free Z-ELP (red) in PBS with added ammonium sulfate. Error bars represent 95% confidence intervals of 3 experiments (* p-value <0.01 difference in T_t > 10 °C, ** p-value <0.01 difference in T_t > 5 °C). (B) Normalized absorbance curve at 350 nm for nanocage (blue triangles) and free Z-ELP (red squares) in PBS without ammonium sulfate. Error bars represent one standard deviation of three experiments.

Although the difference in T_t values decreased with increasing salt concentrations, the significant improvement in transition was preserved for the Z-ELP-E2 nanocages. The global nature of the improvement is ideal for affinity precipitation as this allows more flexibility in selecting salt and temperature conditions that maximize recovery. More importantly, the nanocage transition region occurs within a much sharper temperature range <5 °C compared to over 15 °C for free Z-ELP (Figure 3B). This observation further suggests the feasibility to achieve complete aggregation of Z-ELP-E2 over a smaller temperature range, a condition essential for IgG recovery.

Enhanced Precipitation by Antibody-Inducible Cross-Linking. To confirm the IgG binding capability of Z-ELP-E2 nanocages and to demonstrate the benefit of the lower T_t on IgG recovery, the affinity precipitation process was performed using equal concentrations of either ligated or free Z-ELP and a model polyclonal human IgG at a 5:1 Z:IgG molar ratio. After incubating with IgG for 1 h at 23 °C, the complex was precipitated with varying concentrations of ammonium sulfate at ambient temperature followed by elution with a low pH buffer. Control samples consisting of IgG with ELP-E2 and free ELP (no Z-domain) were employed to test for nonspecific binding. Independent of salt concentration, the Z-ELP-E2 nanocages significantly improved the antibody yields (Figure 4A). In comparison, IgG recovery using free Z-ELP decreased precipitously below 0.5 M ammonium sulfate to negligible recovery with 0.1 M salt. The SDS-PAGE analysis clearly shows that the initial precipitation step was primarily responsible for the IgG yield loss (Supporting Information, Figure S4). More importantly, we demonstrated that the Z-ELP-E2 nanocages can be used to repeatedly capture and elute IgG from a complex mixture of protein impurities with virtually no loss in efficiency (Figure S7).

Interestingly, the IgG−nanocage complex with 0.1 M ammonium sulfate was sufficient to precipitate and elute over 80% of the added IgG at 23 °C. This result cannot be explained simply by the improved transition property as the nanocage T_t is 30 °C in the presence of 0.1 M salt without IgG. It has been shown that ELP domain dimerization can be used to lower the T_t values by increasing the local aggregate size.[24] Because one IgG molecule can bind two Z-domains,[25] a similar dimerization mechanism likely exists. The addition of IgG can potentially act as a cross-linking agent, resulting in network formation between individual Z-ELP-E2 nanoparticles. This hypothesis was verified by detecting an order of magnitude increase in the particle size of Z-ELP-E2 upon the addition of IgG, while no change in particle size was observed for the control ELP-E2 nanoparticles (Figure 4B). Only a small increase in particle size was detected for Z-ELP from 8 to 18 nm, consistent with the formation of smaller localized dimers by IgG cross-linking. Network formation by IgG cross-linking was further confirmed by observing micrometer-sized aggregates by the addition of fluorescently labeled IgGs (Supporting Information, Figure S5). The addition of salt increased the aggregate size for Z-ELP-E2 by approximately 20-fold, corroborated by the small improvement in IgG recovery. However, the presence of salt significantly increased the aggregate size for Z-ELP, resulting in greater than 100-fold larger particles at 0.5 M ammonium sulfate (Figure 4C).

Consistent with the spontaneous cross-linking of Z-ELP-E2 nanoparticles by IgG, complete transition was detected for Z-ELP-E2 even at 20 °C, while the T_t was lowered by 5−6 °C for Z-ELP (Figure 4D). To investigate whether this dramatic decrease in T_t is dependent on the cross-linking density, we evaluated the transition property of a second Z-ELP-E2 conjugate with a significantly lower 35% ligation efficiency. As expected, no visible aggregation was detected upon IgG addition, and the T_t was lowered by a modest 5−6 °C, similar to that in Z-ELP (Figure 4D). This result may be explained by the geometry of the E2 self-assembly. Z-ELP is conjugated to the exterior N-terminus one of the three E2 subunits existing at each of the 20 vertices of the E2 cage spaced ~5 nm apart.[20] At each vertex, it has been suggested that the three E2 monomers make hydrophobic contacts with each other at a distance of

DOI: 10.1021/acs.biomac.7b00275
Biomacromolecules 2017, 18, 1654−1659

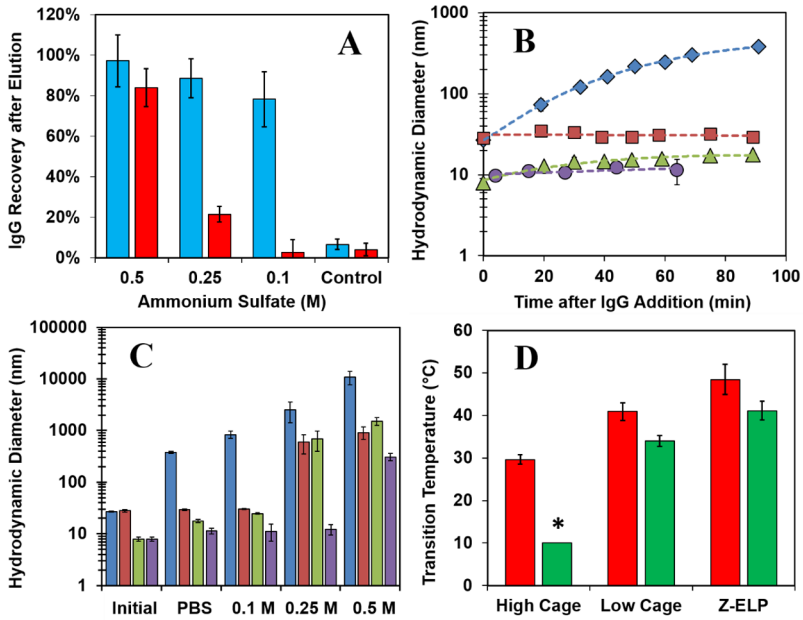

Figure 4. Characterization of antibody affinity precipitation. All experiments used 25 μM ligated Z-ELP on E2 cage at 60% ligation density or 25 μM free Z-ELP with 5 μM polyclonal HIgG. Error bars represent 95% confidence intervals of 3 experiments. (A) Comparison of antibody recovery after elution (in arginine pH 3.7) from nanocage (blue) or Z-ELP (red) using ammonium sulfate for precipitation at 23 °C (* p-value = 0.023, ** p-value < 0.001). Control bars represent ELP-E2 cages or ELPs with no Z-domain using 0.5 M ammonium sulfate for precipitation. (B) DLS size measurements of IgG−nanocage aggregation kinetics at 25 °C in PBS (Z-ELP-E2: blue diamond; ELP-E2: red square; Z-ELP: green triangle; ELP: purple circle) (C) DLS size measurements in PBS at 25 °C of the initial mixture with IgG after a 1 h incubation with IgG and with increasing amounts of ammonium sulfate in PBS (Z-ELP-E2: blue; ELP-E2: red; Z-ELP: green; ELP: purple). (D) Comparison of T_t between 25 μM high ligation Z-ELP-E2 (65%), low ligation Z-ELP-E2 (35%), and free Z-ELP before (red) and 2 h after (green) addition of 5 μM polyclonal HIgG in PBS at 20 °C. * indicates $T_t \ll 20$ °C.

<0.5 nm.[26] A nanocage with 60% ligation density contains an average of two ligated Z-ELP per vertex. Such close proximity may offer an additional cross-linking benefit and may explain why a low ligation cage (35%) with one Z-ELP per vertex behaves more like free Z-ELP (Supporting Information, Figure S6). These observations highlight the importance of localized network formation on the overall transition property of ELP.

Conventional ELP ITC involves the reversible resolubilization at low salt and temperature after precipitation, a property Z-ELP maintains when bound to IgG, reflected by the turbidity measurement (Figure 5). However, because of the substantial cross-linking, IgG bound Z-ELP-E2 precipitates remained insoluble even after 3 days in PBS at 4 °C. This irreversible phase transition enabled the repeated washing in low salt buffers at low temperatures without affecting IgG recovery. Complete resolubilization was observed only after eluting the bound IgG at pH 3.7 (Figure 5), indicating the feasibility to achieve IgG purification by isothermal switching of phase separation.

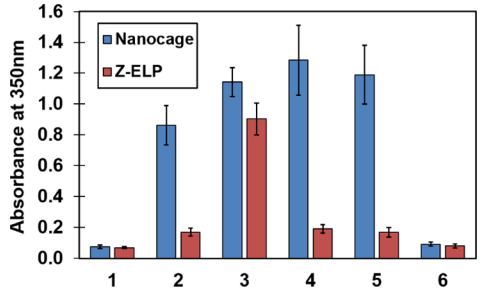

Figure 5. Bound IgG-Z-ELP-E2 complex remained insoluble until elution. Either 25 μM Z-ELP-E2 nanocage at 60% ligation density or 25 μM free Z-ELP was mixed with 5 μM polyclonal HIgG prepared in PBS at 23 °C. Aggregation was reflected by measuring the turbidity at 350 nm. Error bars represent 95% confidence intervals of three experiments. (1) Initial sample before IgG addition. (2) Two-hour incubation at 23 °C. (3) Adjusted to 0.5 M ammonium sulfate. (4) Centrifuged and resuspended back into PBS and incubated at 4 °C for 1 h. (5) Incubated at 4 °C for 3 days. (6) Precipitated again and resuspended in pH 3.7 buffer and incubated at 23 °C for 15 min.

CONCLUSION

In conclusion, we presented a new framework to design enhanced IgG-capturing ELP scaffolds by improving aggregation through increased scaffold dimension and IgG-triggered cross-linking. The ability to induce isothermal switching of phase separation by IgG binding significantly minimized the requirement of salt and eliminated the requirement of a heating step. In addition, the multivalent IgG−nanocage cross-linking yielded stable precipitates, allowing for washing and extended storage in low salt buffers until elution at low pH. Because of the flexibility in tuning the transition property of ELP, it may be possible to achieve complete isothermal separation of IgG using this synthetic purification platform.

ASSOCIATED CONTENT

Supporting Information

The Supporting Information is available free of charge on the ACS Publications website at DOI: 10.1021/acs.biomac.7b00275.

Detailed information on protein expression and purification, SrtA ligation, nanoparticle size characterization, and IgG induced aggregation (PDF)

DOI: 10.1021/acs.biomac.7b00275
Biomacromolecules 2017, 18, 1654−1659

AUTHOR INFORMATION

Corresponding Author

*Fax: (+1) 302-831-1048; Tel: (+1) 302-831-6327; E-mail: wilfred@udel.edu.

ORCID

Wilfred Chen: 0000-0002-6386-6958

Present Address

†Q.S.: Department of Bioengineering, Massachusetts Institute of Technology, Cambridge, Massachusetts 02139, United States.

Notes

The authors declare no competing financial interest.

ACKNOWLEDGMENTS

This work was supported by funding from the NSF (Grant CBET1403724). We would like to acknowledge the Center of Biomedical Research Excellence Microscopy and Mechanical Testing Core (COBRE-MMT) with a grant from the National Institute of General Medical Sciences (NIGMS, Grant 1 P30 GM110758-01) at NIH for use of the Malvern Zetasizer dynamic light scattering instrument.

ABBREVIATIONS

ELP, elastin-like polypeptide; ITC, inverse transition cycling; IgG, immunoglobulin G; mAb, monoclonal antibody; SrtA, Sortase A; FITC, fluorescein isothiocyanate; DLS, dynamic light scattering; TEM, transmission electron microscopy; T_t, transition temperature; IPTG, isopropyl-β-D-thiogalactoside

REFERENCES

(1) Beck, A.; Wurch, T.; Bailly, C.; Corvaia, N. Strategies and challenges for the next generation of therapeutic antibodies. *Nat. Rev. Immunol.* **2010**, *10*, 345−352.

(2) Ecker, D. M.; Jones, S.; Levine, H. L. The therapeutic antibody market. *mAbs* **2015**, *7* (1), 9−14.

(3) Shukla, A. A.; Thömmes, J. Recent advances in large-scale production of monoclonal antibodies and related proteins. *Trends Biotechnol.* **2010**, *28* (5), 253−261.

(4) Ghose, S. M.; Allen, M.; Hubbard, B.; Brooks, C.; Cramer, S. M. Antibody variable region interactions with Protein A: implications for the development of generic purification processes. *Biotechnol. Bioeng.* **2005**, *92* (6), 665−667.

(5) Hillbrig, F.; Freitag, R. Protein Purification by affinity precipitation. *J. Chromatogr. B: Anal. Technol. Biomed. Life Sci.* **2003**, *848* (1), 40−47.

(6) Taipa, M. A.; Kaul, R. H.; Mattiasson, B.; Cabral, J. M. S. Recovery of a monoclonal antibody from hybridoma culture supernatant by affinity precipitation with Eudragit S-100. *Bioseparation* **2000**, *9* (5), 291−298.

(7) Takei, Y. G.; Aoki, T.; Sanui, K.; Ogata, N.; Sakurai, Y.; Okano, T.; Matsukata, M.; Kikuchi, A. Temperature-responsive bioconjugates. 3. Antibody-Poly(N-isopropylacrylamide) conjugates for temperature-modulated precipitations and affinity bioseparations. *Bioconjugate Chem.* **1994**, *5* (6), 577−582.

(8) Kowalczyk, T.; Hnatuszko-Konka, K.; Gerszberg, A.; Kononowicz, A. K. Elastin-like polypeptides as a promising family of genetically-engineered protein based polymers. *World J. Microbiol. Biotechnol.* **2014**, *30* (8), 2141−2152.

(9) Chilkoti, A.; Christensen, T.; MacKay, J. A. Stimulus responsive elastin biopolymers: applications in medicine and biotechnology. *Curr. Opin. Chem. Biol.* **2006**, *10* (6), 652−657.

(10) Kim, J. Y.; Mulchandani, A.; Chen, W. Temperature-triggered purification of antibodies. *Biotechnol. Bioeng.* **2005**, *90*, 373−379.

(11) Lao, U. L.; Mulchandani, A.; Chen, W. Simple Conjugation and Purification of Quantum Dot-Antibody Complexes Using a Thermally Responsive Elastin-Protein L Scaffold As Immunofluorescent Agents. *J. Am. Chem. Soc.* **2006**, *128*, 14756−14757.

(12) Liu, F.; Chen, W. Engineering a recyclable ELP capturing scaffold for non-chromatographic protein purification. *Biotechnol. Prog.* **2013**, *29*, 968−971.

(13) Kim, H.; Chen, W. A non-chromatographic protein purification strategy using src 3 homology domains as generalized capture domains. *J. Biotechnol.* **2016**, *234*, 27−34.

(14) Madan, B.; Chaudhary, G.; Cramer, S. M.; Chen, W. ELP-z and ELP-zz capturing scaffolds for the purification of immunoglobulins by affinity precipitation. *J. Biotechnol.* **2013**, *163* (1), 10−16.

(15) Sheth, R. D.; Madan, B.; Chen, W.; Cramer, S. M. *Biotechnol. Bioeng.* **2013**, *110*, 2664−2676.

(16) Sheth, R. D.; Jin, M.; Bhut, B. V.; Liu, J.; Lee, J.; Siegfried, R.; Li, Z.; Chen, W.; Cramer, S. M. Affinity precipitation of a monoclonal antibody from an industrial harvest feedstock using an ELP-Z stimuli responsive biopolymer. *Biotechnol. Bioeng.* **2014**, *111*, 1595−1603.

(17) Arosio, P.; Jaquet, B.; Wu, H.; Morbidelli, M. On the role of salt type and concentration on the stability behavior of a monoclonal antibody solution. *Biophys. Chem.* **2012**, *168*, 19−27.

(18) Mirica, K. A.; Lockett, M. R.; Snyder, P. W.; Shapiro, N. D.; Mack, E. T.; Nam, S.; Whitesides, G. M. Selective precipitation and purification of monovalent proteins using oligovalent ligands and ammonium sulfate. *Bioconjugate Chem.* **2012**, *23* (2), 293−299.

(19) Handlogten, M. W.; Stefanick, J. F.; Alves, N. J.; Bilgicer, B. Nonchromatographic Affinity Precipitation Method for the Purification of Bivalently Active Pharmaceutical Antibodies from Biological Fluids. *Anal. Chem.* **2013**, *85* (10), 5271−5278.

(20) Chen, Q.; Sun, Q.; Molino, N. M.; Wang, S.-W.; Boder, E. T.; Chen, W. Sortase A-mediated multi-functionalization of protein nanoparticles. *Chem. Commun.* **2015**, *51*, 12107−12110.

(21) Levary, D. A.; Parthasarathy, R.; Boder, E. T.; Ackerman, M. E. Protein-Protein Fusion Catalyzed by Sortase A. *PLoS One* **2011**, *18*, 469−476.

(22) Sun, Q.; Chen, Q.; Blackstock, D.; Chen, W. Post-translational modification of bio-nanoparticles as a modular platform for biosensor assembly. *ACS Nano* **2015**, *9* (8), 8554−8561.

(23) Zhou, H. Z.; Liao, W.; Cheng, R. H.; Lawson, J. E.; McCarthy, D. B.; Reed, L. J.; Stoops, J. K. Direct Evidence for the Size and Conformational Variability of the Pyruvate Dehydrogenase Complex Revealed by Three-dimensional Electron Microscopy. *J. Biol. Chem.* **2001**, *276* (15), 21704−21713.

(24) Dhandhukia, J.; Weitzhandler, I.; Wang, W.; MacKay, J. A. Switchable elastin-like polypeptides that respond to chemical inducers of dimerization. *Biomacromolecules* **2013**, *14* (4), 976−985.

(25) Jendeberg, L.; Persson, B.; Andersson, R.; Karlsson, R.; Uhlen, M.; Nilsson, B. Kinetic analysis of the interaction between protein a domain variants and human Fc using plasmon resonance detection. *J. Mol. Recognit.* **1995**, *8* (4), 270−278.

(26) Hezaveh, S.; Zeng, A.-P.; Jandt, U. Human Pyruvate Dehydrogenase Complex E2 and E3BP Core Subunits: New Models and Insights from Molecular Dynamics Simulations. *J. Phys. Chem. B* **2016**, *120* (19), 4399−4409.

DOI: 10.1021/acs.biomac.7b00275
Biomacromolecules 2017, 18, 1654−1659